

01 Aug 2020

Effects Of Clay Creep On Long-Term Load-Carrying Behaviors Of Bored Piles: Aiming At Reusing Existing Bored Piles

Lin Li

Weibing Gong

Missouri University of Science and Technology, weibing.gong@mst.edu

Jingpei Li

Jingpei Li

Follow this and additional works at: https://scholarsmine.mst.edu/geosci_geo_peteng_facwork



Part of the [Geological Engineering Commons](#)

Recommended Citation

L. Li et al., "Effects Of Clay Creep On Long-Term Load-Carrying Behaviors Of Bored Piles: Aiming At Reusing Existing Bored Piles," *International Journal of Geomechanics*, vol. 20, no. 8, article no. 04020132, American Society of Civil Engineers, Aug 2020.

The definitive version is available at [https://doi.org/10.1061/\(ASCE\)GM.1943-5622.0001769](https://doi.org/10.1061/(ASCE)GM.1943-5622.0001769)

This Article - Journal is brought to you for free and open access by Scholars' Mine. It has been accepted for inclusion in Geosciences and Geological and Petroleum Engineering Faculty Research & Creative Works by an authorized administrator of Scholars' Mine. This work is protected by U. S. Copyright Law. Unauthorized use including reproduction for redistribution requires the permission of the copyright holder. For more information, please contact scholarsmine@mst.edu.



Effects of Clay Creep on Long-Term Load-Carrying Behaviors of Bored Piles: Aiming at Reusing Existing Bored Piles

Lin Li¹; Weibing Gong, S.M.ASCE²; and Jingpei Li³

Abstract: An analytical procedure is presented for assessing the long-term load-carrying behavior of bored piles in clay, where the plastic volumetric strain of surrounding clay caused by creep is estimated by an advanced elasto-viscoplastic constitutive model. Two key soil parameters, the undrained shear strength and the shear modulus, which govern the load-carrying behavior of bored piles in clay, are determined from the definition of the quasi-overconsolidation ratio and the concept of the critical state theory-based Cam-clay model. The long-term load-carrying capacity of bored piles is evaluated based on the total stress method. Hyperbolic load-transfer models are developed with proper incorporation of the two developed soil parameters to predict the long-term load–settlement behaviors of the bored pile. The proposed framework is validated by predicting a pile field test on an existing bored pile (about 30 years) in clay, which was recently performed by the authors in Pudong New Area, Shanghai, and field static load tests on two single bored piles conducted by other researchers. Comprehensive parametric studies are conducted to explore the effects of secondary compression index and in situ soil properties on long-term load-carrying behavior of bored piles. The proposed procedure is expected to provide useful guidance for estimating the load-carrying behavior of existing bored piles in clay and take the ultimate aim of reusing them in practice. DOI: 10.1061/(ASCE)GM.1943-5622.0001769. © 2020 American Society of Civil Engineers.

Author keywords: Long-term; Load-carrying behavior; Creep; Quasi-overconsolidation ratio; Existing bored pile.

Introduction

With the fast urbanization in China, more and more existing buildings, especially in those large and densely populated cities, such as Shanghai and Beijing, can barely meet the using requirements of current life. Therefore, a large number of these buildings have been demolished but with many piles left in situ. Among these piles, the bored piles take an important place, due to the advantages that they can avoid the vibration of a pile hammer and eliminate the damages to adjacent structures; in addition, they make it easy to adjust the depth for suiting various soil conditions. Faced with the existing bored piles, geotechnical engineers usually own two methods to deal with them. One is to remove them directly from the construction sites, but it will cause great disturbance on soil and, on the other hand, will largely increase construction costs. The other is to reuse them when constructing new buildings. It is obvious that the reuse method retains competitive advantages compared with the removal method, because it is time-saving, economical, and environmental-friendly. In light of the advantages of the reuse method, it is quite significant and necessary to clearly understand the load-carrying behaviors of existing bored piles. To achieve this aim, exploring the long-term load-carrying behaviors of bored piles naturally becomes the prime goal, because the

existing bored piles have generally existed in the construction sites for over 20 years or even more.

Up to now, great efforts have been dedicated to exploring the load-carrying behaviors of piles in clay (e.g., Ashour et al. 2010; Basu et al. 2014; Li et al. 2017a, b, c; Xia and Zou 2017). Some of these efforts primarily focus on the time-dependent load-carrying behaviors. For example, Flaate (1972) summarized the information about mechanical properties of the surrounding clay after pile installation based on field observations and measurements so as to better understand the continuous increase of skin friction of driven piles; Randolph and Wroth (1979a) derived an analytical solution to the subsequent consolidation of the clay around a driven pile to study the dissipation of excess pore-water pressure and further to explore the increase of bearing capacity of the pile after installation; Roy and Lemieux (1986) conducted an in situ test on long-term behaviors of the reconsolidated clay around a pile to investigate the mechanism of time-dependent load-carrying behaviors of the pile; Guo (2000) predicted the overall response of a driven pile following installation and the solution successfully incorporated the viscosity of soft clays. More recently, Li et al. (2017a, c) proposed an effective stress-based analytical approach and adopted the total stress method to evaluate the time-dependent bearing capacity of a driven pile in clayey soils; Li et al. (2017b) also presented a semianalytical approach to predict the time-dependent load–settlement response of a jacked pile in clay strata. From the aforementioned literature, it can be found that most of the available research studies focused on the time-dependent load-carrying behaviors of displacement piles while excluded bored piles. This may be because the displacement piles exhibit the strong setup effect, which results from the dissipation of installation-induced excess pore-water pressure. However, it should be worth noting that the clay creep may also make great contributions to the pile setup (Tavenas and Audy 1972; Schmertmann 1991), which primarily accounts for the time-dependent load-carrying behaviors of bored piles after construction in clay (particular referring to the long-term load-carrying behaviors), although there is no (or

¹Dept. of Geotechnical Engineering, Tongji Univ., Shanghai 200092, China. Email: lilin_sanmao@163.com

²Dept. of Geotechnical Engineering, Tongji Univ., Shanghai 200092, China (corresponding author). Email: 12weibing_gong@tongji.edu.cn

³Dept. of Geotechnical Engineering, Tongji Univ., Shanghai 200092, China; Key Laboratory of Geotechnical and Underground Engineering, Ministry of Education, Tongji Univ., Shanghai 200092, China. Email: lij2773@tongji.edu.cn

Note. This manuscript was submitted on February 15, 2019; approved on March 24, 2020; published online on June 8, 2020. Discussion period open until November 8, 2020; separate discussions must be submitted for individual papers. This paper is part of the *International Journal of Geomechanics*, © ASCE, ISSN 1532-3641.

very little, which is negligible) excess pore-water pressure generated during the construction of bored piles.

Therefore, to facilitate the reuse of existing bored piles, this paper proposes an analytical framework to explore the effects of clay creep on long-term load-carrying behaviors of bored piles. For this, a sophisticated elasto-viscoplastic constitutive model is employed to estimate the decrease in the void ratio of surrounding clay, which is the prime factor causing a quasi-overconsolidated effect of clay. Two key soil parameters, the undrained shear strength and the shear modulus, which govern the load-carrying behaviors of piles in clay, are determined from the definition of the quasi-overconsolidation ratio and the concept of the critical state theory-based Cam-clay model. The long-term load-carrying capacity of a bored pile in clay is evaluated in terms of the total stress method. The hyperbolic nonlinear models are developed with the incorporation of the effects of clay creep to simulate the load-transfer behaviors of the pile shaft and end, based on which the analytical framework is proposed to estimate the long-term load-settlement behaviors of a bored pile in clay. The validity of the proposed framework is examined by predicting a field test conducted by the authors in Shanghai and field static load tests on two individual bored piles conducted by Dai et al. (2012). With the proposed analytical framework, parametric studies are conducted to investigate the effects of the secondary compression index and in situ soil properties on the long-term load-carrying behaviors of bored piles in clay.

Effects of Clay Creep

In the actual situation, the clay around the bored piles first undergoes primary consolidation under the load transferred from the superstructure. At the same time, secondary consolidation due to clay creep occurs. After the primary consolidation, the clay around bored piles primarily undergoes the secondary consolidation with the passage of time. In this phrase, the deformation occurring in the soil skeleton is mainly caused by pure creep (Augustesen et al. 2004). In other words, after the primary consolidation, the deformation of the surrounding clay chiefly results from the creep. The creep deformation leads to the occurrence of the plastic volumetric strain of the surrounding clay, which affects the undrained shear strength and the shear modulus of the surrounding clay and further exerts influences on the long-term load-carrying behavior of a bored pile in clay. Because this study primarily focuses on the long-term load carry behavior of bored piles caused by the clay creep, the process of the primary consolidation is beyond the scope and thus has not been discussed in detail herein. Nevertheless, the actual stress state of soil at different depths along the pile shaft under the working load after the primary consolidation is determined through the load-transfer method so as to model and analyze the creep behavior of surrounding clay, which will be shown subsequently in the paper.

Due to pile construction effects, the clay around bored piles is remolded and exhibits the mechanical properties similar to normally consolidated clays (Randolph and Wroth 1981). Thus, an advanced elasto-viscoplastic constitutive model for normally consolidated clays (Sekiguchi 1984), which is developed based on the Cam-clay model, can be employed to describe the creep of the surrounding clay. This model can accurately predict the non-linear nature of the clay creep. The potential function, F , of this constitutive model is expressed as follows (Sekiguchi 1984):

$$F \equiv e_v^p = \xi \ln \left[1 + \frac{\dot{\epsilon}_0 t}{\xi} \exp \left(\frac{f}{\xi} \right) \right] \quad (1)$$

where ξ = secondary compression index; $\dot{\epsilon}_0$ = reference volumetric strain; t = elapsed time; and the function, f , is written as follows:

$$f = \frac{\lambda - \kappa}{1 + e_0} \ln \left(\frac{p'_p}{p'_0} \right) + D \left(\frac{q_p}{p'_p} - \frac{q_0}{p'_0} \right) \quad (2)$$

where λ = compression index; and κ = swelling index, whose definitions are depicted in Fig. 1; e_0 = initial void ratio; p'_0 and q_0 = initial mean effective stress and initial deviator stress of in situ clay, respectively; p'_p and q_p = mean effective stress and deviator stress of the surrounding clay when an axial load is applied to the pile head; and D = coefficient of dilatancy, which can be determined from the following equation (Sekiguchi 1984):

$$D = \frac{\lambda - \kappa}{M(1 + e_0)} \quad (3)$$

where M = slope of the critical state line, equal to

$$M = \frac{6 \sin \phi'}{3 - \sin \phi'} \quad (4)$$

where ϕ' = effective friction angle.

The creep leads to only the plastic deformation of the clay, and thus for a bored pile under constant working loads, the plastic volumetric strain of the surrounding clay induced by creep is equal to the total volumetric strain, i.e., $\epsilon_v^p = \epsilon_v$. The increase of creep plastic volumetric strain leads to the decrease of the void ratio of the surrounding clay, and the decrease of the void ratio can be regarded to be caused by the increase of equivalent preconsolidation pressure, p'_{ec} (Bjerrum 1967; Augustesen et al. 2004). Fig. 2 well illustrates this phenomenon. As shown in the figure, the aged clay undergoes significant secondary compression (decreases in the void ratio) at constant effective stress. Correspondingly, the measured preconsolidation pressure of aged clay increases from the preconsolidation pressure of new clay, p'_{c0} , to its own preconsolidation pressure, p'_{c1} . The larger preconsolidation pressure indicates a more stable clay structure. On the other hand, the increase of equivalent preconsolidation pressure corresponds to the variation of the location of preconsolidation pressure on the isotropic compression line in the modified Cam-clay model.

As shown in Fig. 1, the total volumetric strain is easily determined from the relationship in the $e - \ln p'$ plane. Hence, the

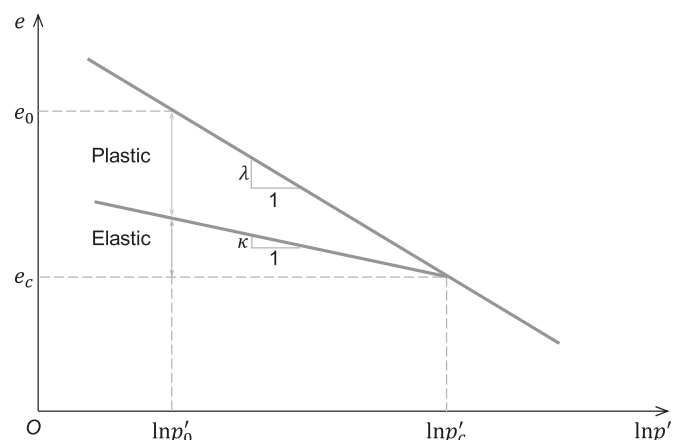


Fig. 1. Definition of compression and swelling indexes.

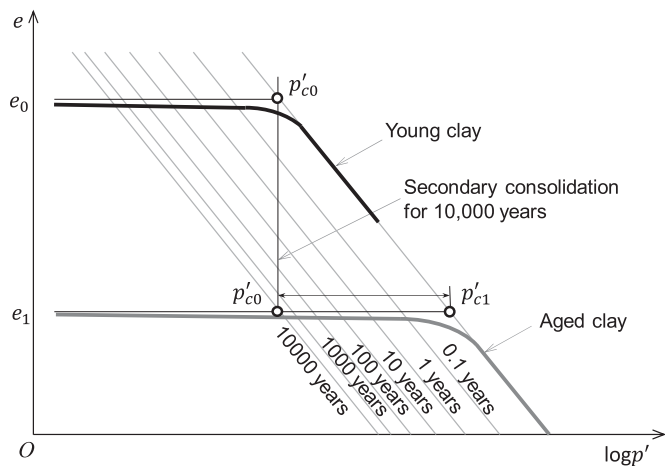


Fig. 2. Compression curves of young and aged clays.

creep plastic volumetric strain can be obtained as follows:

$$\epsilon_v^p = \epsilon_v = \frac{\lambda}{1 + e_0} \ln \left(\frac{p'_{ec}}{p'_p} \right) \quad (5)$$

Combining Eqs. (1) and (5) yields

$$\frac{p'_{ec}}{p'_p} = \exp \left\{ \frac{(1 + e_0)\xi}{\lambda} \ln \left[1 + \frac{\dot{\epsilon}_0 t}{\xi} \exp \left(\frac{f}{\xi} \right) \right] \right\} \quad (6)$$

From the preceding equation, it can be found that the equivalent preconsolidation pressure increases with the elapse of time, which leads to the surrounding clay displaying the quasi-overconsolidated behaviors. To quantitatively explore the gradual changes in the mechanical properties of surrounding clay as well as the long-term load-carrying behaviors of bored piles in clay, a coefficient, which is referred to as the quasi-overconsolidation ratio, is defined in the following equation:

$$R = \exp \left\{ \frac{(1 + e_0)\xi}{\lambda} \ln \left[1 + \frac{\dot{\epsilon}_0 t}{\xi} \exp \left(\frac{f}{\xi} \right) \right] \right\} \quad (7)$$

From Eq. (7), it can be seen that the quasi-overconsolidation ratio increases with the elapse of time. This indicates that the surrounding clay displays stronger quasi-overconsolidated behaviors when the time for secondary consolidation becomes longer.

Gradual Changes in Mechanical Properties of Surrounding Clay

The in situ undrained shear strength of clay, s_{u0} , can be defined based on the concept of the modified Cam-clay model as follows (Wood 1990):

$$s_{u0} = \frac{1}{2} M p'_0 \left(\frac{\text{OCR}}{2} \right)^\Lambda \quad (8)$$

where OCR = overconsolidation ratio; and $\Lambda (=1 - \kappa/\lambda)$ = plastic volumetric strain ratio. Due to the pile construction effects, the clay around bored piles exhibits the mechanical behaviors similar to the normally consolidated clay. Thus, the OCR of the surrounding clay can be taken as unity after bored pile construction (Randolph and Wroth 1981; Yao et al. 2009). However, due to the clay creep, the aged clay reveals the quasi-overconsolidated behaviors (see Fig. 2). This creep-induced increase of quasi-overconsolidation

ratio corresponds to the increase of consolidation stress of normally consolidated clay in the modified Cam-clay model. Hence, the undrained shear strength of the surrounding clay after bored pile construction, s_u , which incorporates the construction effects and clay creep, can be given by

$$s_u(t) = MR p'_p \left(\frac{1}{2} \right)^{\Lambda+1} \quad (9)$$

The shear modulus of the surrounding clay, as the other important mechanical parameter that has significant influences on the load-carrying behaviors of a bored pile, can be defined as follows (Matsuoka and Sun 2006):

$$G = \frac{3(1 - 2\nu')\nu p'}{2\kappa(1 + \nu')} \quad (10)$$

where ν' = effective void ratio; and $\nu (=1 + e)$ = specific volume.

Note that the volumetric strain, ϵ_v , can also be expressed in terms of the variation of void ratio, i.e.,

$$\epsilon_v = -\frac{e - e_0}{1 + e_0} \quad (11)$$

Then, the variation in the void ratio of the surrounding clay caused by the clay creep can be derived by substituting Eq. (1) into Eq. (11) as follows:

$$e = e_0 - \xi(1 + e_0) \ln \left[1 + \frac{\dot{\epsilon}_0 t}{\xi} \exp \left(\frac{f}{\xi} \right) \right] \quad (12)$$

From Eq. (12), it can be seen that the void ratio of surrounding clay decreases with the elapse of time, which well reflects the increase in the plastic deformation of surrounding clay caused by clay creep.

Substituting Eqs. (6) and (12) into Eq. (10), the shear modulus of the surrounding clay, which takes the clay creep into consideration, can be taken as follows:

$$G(t) = \frac{3(1 - 2\nu')(1 + e_0 - \lambda \ln R) p'_p R}{2\kappa(1 + \nu')} \quad (13)$$

Eqs. (9) and (13) demonstrate that the undrained shear strength and the shear modulus of clay around bored piles after construction increase with the elapse of time due to the effects of clay creep, which properly explains the primary cause for the time-dependent load-carrying behaviors of a bored pile in clay (especially referring to the long-term load-carrying behavior).

Long-Term Axial Load-Carrying Capacity of a Bored Pile in Clay

Compared with the effective stress method and the piezocone penetration test method, the total stress method is much simpler when employed to evaluate the load-carrying capacity of a bored pile in clay (Wardle et al. 1992; Li et al. 2017b), due to the easier determination of calculation parameters in this method. Hence, it is applied herein to estimate the pile end resistance and the pile shaft resistance. When applying the total stress method to estimate the long-term bearing capacity of a bored pile in clay, the key task lies in determining both the long-term pile end bearing capacity factor, $N_c(t)$, and the long-term pile shaft resistance factor, $\alpha(t)$. The unit end bearing resistance of a pile in clay can be evaluated in terms

of the total stress method as follows:

$$q_b = N_c s_{u0} \quad (14)$$

where N_c = end bearing capacity factor and empirically considered to be 9 (Wardle et al. 1992). Taking the time-dependent effects resulting from clay creep into consideration, the long-term unit end bearing resistance of the bored pile in clay can be given as follows:

$$q_b(t) = N_c(t) s_{u0} \quad (15)$$

where $N_c(t)$ = long-term end bearing capacity factor, equal to

$$N_c(t) = N_c \frac{s_u(t)}{s_{u0}} = N_c \frac{R}{OCR^\Lambda} \quad (16)$$

Then, the long-term total pile end bearing capacity can be easily obtained as follows:

$$Q_b(t) = \pi r_p^2 q_b(t) \quad (17)$$

where r_p = pile radius.

Fig. 3 illustrates the schematic of an axially loaded pile. As shown in the figure, the stress state of a soil element adjacent to the pile shaft is approximately equivalent to that of a soil sample in a simple shear test, in which the horizontal shear stress, τ_{yx} , and the unit pile shaft resistance, f_s , can be expressed in terms of the undrained shear strength under the plane strain condition, s_{up} , as follows (Randolph and Wroth 1981; Li et al. 2017b):

$$f_s = \tau_{yx} = s_{up} \cos \varphi' \quad (18)$$

Note that the developed undrained shear strength in Eq. (9), which incorporates the effects of clay creep, is defined under the triaxial stress state. It is obvious that the undrained shear strength under the triaxial compression condition is different from that under the plane strain condition, due to its inherent three-dimensional mechanical properties. Hence, in order to determine the unit pile shaft resistance, the developed undrained shear strength under the triaxial compression condition should be related to the undrained shear strength under the plane strain condition. This can be easily achieved by the stress-transformed method integrated with the spatially mobilized plane criterion proposed by Matsuoka et al. (1999) in the following:

$$s_{up} = \frac{3 \sin \Psi_f}{M \sqrt{2 + \sin^2 \Psi_f}} s_u \quad (19)$$

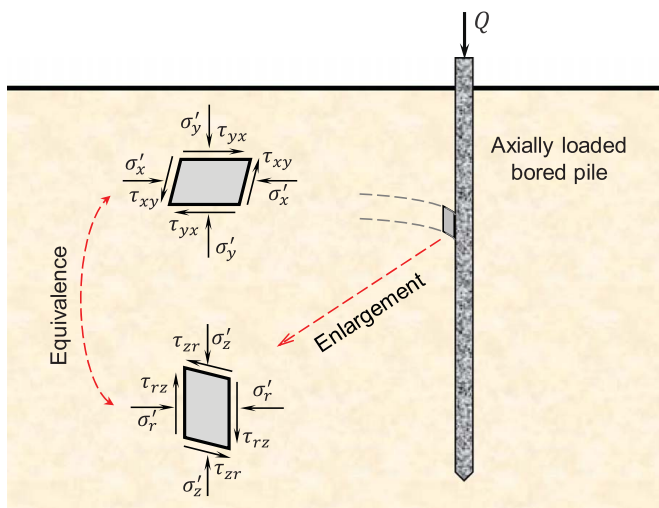


Fig. 3. Schematic of an axially loaded bored pile in clay.

where the stress-transformed parameter, Ψ_f , is expressed as follows:

$$\sin \Psi_f = \frac{\sqrt{2} M}{\sqrt{9 + 3M}} \quad (20)$$

Substitution of Eqs. (8), (9), and (19) into Eq. (18) gives the long-term unit pile shaft resistance in the following:

$$f_s(t) = \frac{3 \sin \Psi_f \cos \varphi'}{M \sqrt{2 + \sin^2 \Psi_f}} \frac{R}{OCR^\Lambda} s_{u0} \quad (21)$$

Similar to the derivation of the long-term unit end bearing resistance, the long-term unit pile shaft resistance, incorporating the effects of clay creep, can also be expressed in terms of the total stress method as follows:

$$f_s(t) = \alpha(t) s_{u0} \quad (22)$$

Comparing Eq. (21) with Eq. (22), the long-term pile shaft resistance factor, $\alpha(t)$, can be written as follows:

$$\alpha(t) = \frac{3 \sin \Psi_f \cos \varphi'}{M \sqrt{2 + \sin^2 \Psi_f}} \frac{R}{OCR^\Lambda} \quad (23)$$

When the long-term unit pile shaft resistance is determined, the long-term total pile shaft bearing capacity can be estimated as follows:

$$Q_s(t) = \int_0^L 2\pi r_p f_s(t) dz \quad (24)$$

where L = pile length.

It is easily known that the total load-carrying capacity of an axially loaded pile consists of the total pile end bearing capacity and the total pile shaft bearing capacity. Thus, the total long-term total bearing capacity of a bored pile in clay can be calculated as follows:

$$Q(t) = Q_s(t) + Q_b(t) = \int_0^L 2\pi r_p f_s(t) dz + \pi r_p^2 q_b(t) \quad (25)$$

When the existing time of the bored pile in clay is given, its corresponding total load-carrying capacity at the given time can be estimated from Eq. (25).

Long-Term Load–Settlement Behavior of a Pile in Clay

The relationship between the pile shaft shear stress and the corresponding pile–soil relative displacement has been widely explored through both laboratory and field tests. The well-documented test results (e.g., Zhao et al. 2009; Zhang and Zhang 2012) indicate that a hyperbolic function-based load-transfer curve can be harnessed to describe the nonlinear behavior of the pile–soil interface during pile loading. Hence, a nonlinear hyperbolic model is also adopted in this study to describe the nonlinear behavior of the pile–soil interface, and the model can be written as follows (Zhang and Zhang 2012):

$$\tau_s(z) = \frac{S_s(z)}{a_s + b_s S_s(z)} \quad (26)$$

where $S_s(z)$ = corresponding pile–soil relative displacement; $\tau_s(z)$ = pile shaft shear stress at depth, z ; and a_s and b_s = initial stiffness and reciprocal of the asymptote of the pile shaft load-transfer curve (see Fig. 4), respectively.

The back-analysis of field tests or laboratory tests is a rational way to determine the parameters in the hyperbolic nonlinear model. However, the back-analysis method is not only time-consuming, but also unable to incorporate the creep-induced changes in mechanical

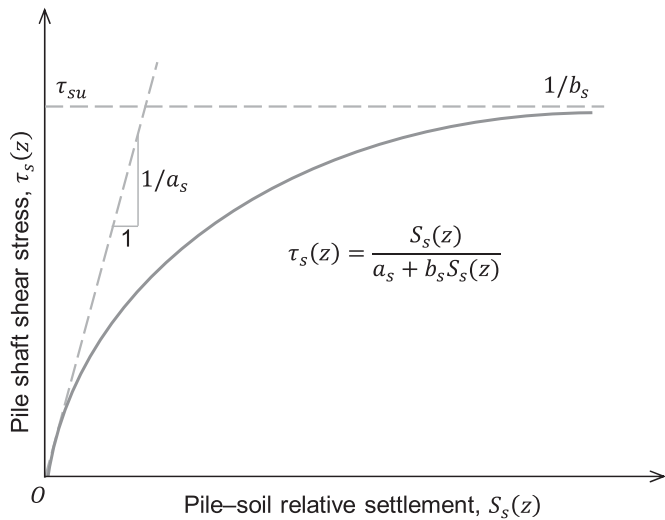


Fig. 4. Hyperbolic relationship between unit shear stress and pile settlement at the pile-soil interface.

properties of the surrounding clay. Here, an alternative theoretical approach is adopted to determine the model parameters based on their mechanical meanings. From Fig. 4, it can be observed that the parameter a_s denotes the initial stiffness of the pile shaft load-transfer curve and its value can be determined as follows (Randolph and Wroth 1979b):

$$a_s = \frac{r_p}{G_s} \ln\left(\frac{r_m}{r_p}\right) \quad (27)$$

where $r_m [=2.5L(1 - \nu)]$ is the limiting influence radius of the pile, beyond which the induced pile shaft shear stress is negligible. The parameter b_s denotes the reciprocal of the asymptote of the pile shaft load-transfer curve, and its value can be given by

$$b_s = \frac{1}{\tau_{su}} = \frac{1}{f_s} \quad (28)$$

Assuming that the pile end load-settlement behavior also follows the hyperbolic nonlinear relationship (see Fig. 5), the unit pile end resistance, q_b , can be written as follows:

$$q_b = \frac{S_b}{a_b + b_b S_b} \quad (29)$$

where S_b = pile end settlement.

Similar to the determination of parameters in the nonlinear hyperbolic model for the pile shaft, the parameters in the model for the pile end are also determined based on the corresponding parameter meanings. The parameter a_b denotes the initial stiffness of the pile end load-transfer curve, which can be derived as follows (Randolph and Wroth 1979b):

$$a_b = \frac{(1 - \nu)\pi r_p}{4G_b} \quad (30)$$

and b_b = ultimate pile base resistance, given by

$$b_b = \frac{1}{q_{bu}} = \frac{1}{N_c S_{u0}} \quad (31)$$

Algorithms for Analysis

The soil elements along the pile shaft show different stress states under the working load after the primary consolidation, which causes

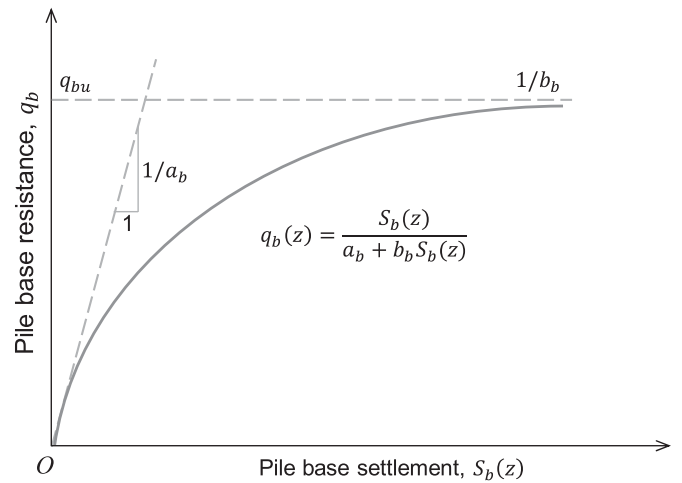


Fig. 5. Hyperbolic relationship between unit end resistance and pile end settlement.

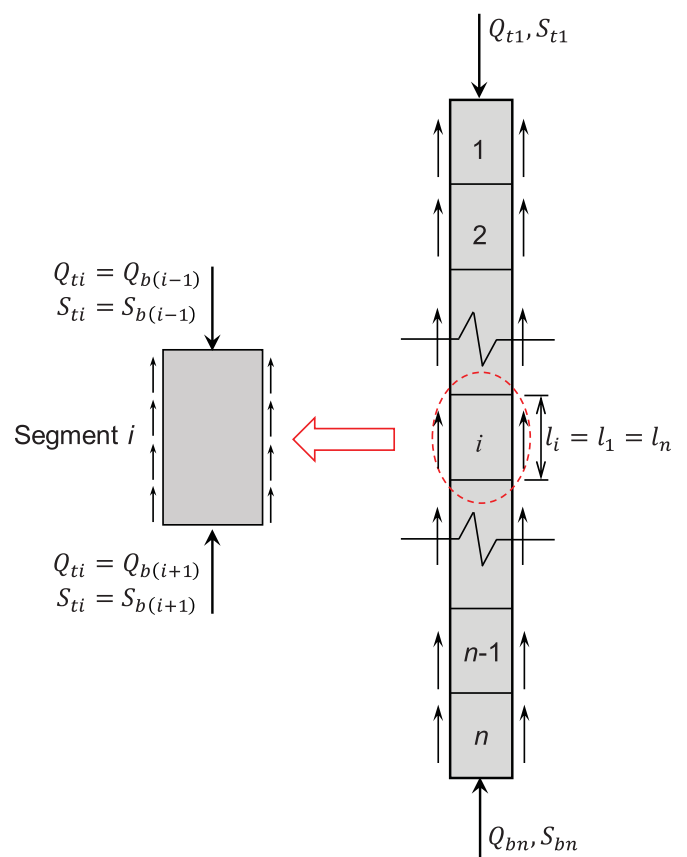


Fig. 6. Discretization of an axially loaded pile.

different creep behaviors of the clay along the pile shaft. To consider the effect of the primary consolidation caused by the load transferred from the superstructure, the load-transfer method is employed to determine the stress states of the surrounding clay after the primary consolidation to simulate and determine the creep behavior of the surrounding clay. It is shown in Fig. 6 that the pile is equally discretized into n small segments along the pile shaft, which guarantees that the shear stress along the shaft of a small pile segment can be assumed as a constant value. When the load applied to the pile head, Q_b , is known, it is easy to calculate the shaft shear stress of every pile element, τ_{si} . Then, the stress state of the soil element

adjacent to the pile under the working load after the primary consolidation can be determined as follows:

$$\sigma'_{1i} = \frac{\sigma'_{r0i} + \sigma'_{z0i}}{2} + \sqrt{\tau_{si}^2 + \frac{(\sigma'_{r0i} - \sigma'_{z0i})^2}{4}} \quad (32)$$

$$\sigma'_{2i} = \frac{\sigma'_{r0i} + \sigma'_{z0i}}{2} - \sqrt{\tau_{si}^2 + \frac{(\sigma'_{r0i} - \sigma'_{z0i})^2}{4}} \quad (33)$$

$$\sigma'_{3i} = \sigma'_{\theta 0i} \quad (34)$$

Correspondingly, the mean effective stress, p'_{pi} , and the deviator stress, q_{pi} , of the soil element, i , which consider the effect of axial loading of the pile, can be written as follows:

$$p_{pi} = \frac{1}{3}(\sigma'_{1i} + \sigma'_{2i} + \sigma'_{3i}) \quad (35)$$

$$q_{pi} = \sqrt{\frac{1}{2}[(\sigma'_{1i} - \sigma'_{2i})^2 + (\sigma'_{1i} - \sigma'_{3i})^2 + (\sigma'_{2i} - \sigma'_{3i})^2]} \quad (36)$$

Substitution of Eq. (2), along with Eqs. (35) and (36), into Eq. (7) allows for the determination of the function of the

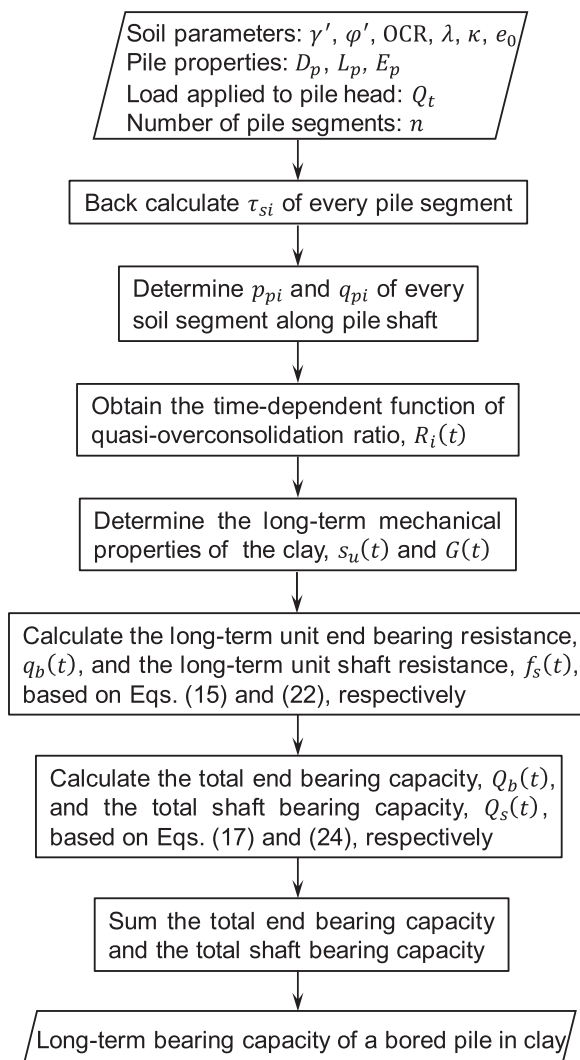


Fig. 7. Procedures for determining long-term load-carrying capacity of a bored pile in clay.

quasi-overconsolidation ratio varying with respect to time. Algorithms are elaborately conceived to predict the long-term load-carrying behaviors of a bored pile existing for different decades after construction. The specific procedures of algorithms for exploring the long-term load-carrying behaviors of a bored pile in clay are shown in Figs. 7 and 8. Following the procedures, calculation codes are developed with MATLAB 2018b, which only cost several seconds to predict the long-term load-carrying behavior of a bored pile in clay existing for different decades.

Validation and Parametric Study

To verify the proposed analytical framework, a pile field test was conducted by the authors in Pudong New Area of Shanghai to investigate the load–settlement behavior of an existing bored pile in clay. The test site used to be a factory, where the superstructures were demolished but with many bored piles left in situ. Faced with the existing bored piles, the engineers once considered removing them directly from the site. However, it was evaluated that the removal would largely increase the total construction costs. Moreover, the removal would cause great disturbance in the surrounding clay, which may increase the difficulty in constructing new piles. Hence, the load–settlement behavior of an existing bored pile at the test site was measured with the aim of reusing the existing piles. The tested bored pile has existed in the construction sites for almost 30 years. It has a length of 29 m and a circular section with a diameter, d , of 500 mm. The elastic modulus of the tested bored pile was determined based on the transformed area method (O’Neil and Reese 1999; Lam and Jefferis 2011), which is one of the methods popularly adopted in design manuals. Through assuming force equilibrium between the reinforcing bars and the concrete in a pile cross section and strain compatibility, the axial stiffness of bored piles can be estimated as $EA = E_c A_c + E_s A_s$, where E , E_c , and E_s , together with A , A_c , and A_s , are the elastic moduli and cross-sectional areas of bored pile, concrete, and reinforcing bars, respectively. The preceding equation can be used to estimate the elastic modulus of bored piles, when the elastic moduli and cross-sectional areas of concrete and reinforcing bars are known. Based on the construction records of bored piles, the respective cross-sectional areas of reinforcing bars and concrete as well as the elastic modulus of reinforcing bars were easily determined. The elastic modulus of concrete was measured on cylinder specimens taken from another in situ bored pile that was casted using the same construction method. After the determination of elastic moduli and cross-sectional areas of the concrete and reinforcing bars, the elastic modulus of the bored pile was estimated using the preceding equation as 30 GPa. The total load was applied step-by-step to the pile head with an increment of 180 kN, and the first load applied to the pile head was 360 kN. Every load step lasted for 2 h, and the settlements at the pile head were recorded at 5, 15, 30, 45, 60, 90, and 120 min. The load that the pile used to bear and produced by the superstructures is evaluated as 800 kN.

The soil strata at the test site are mainly composed of soft clay, clayey silt, mucky clay, and silty clay with the layer thicknesses of 3.3, 3.9, 9.4, and 20 m, respectively. The soils are normally overconsolidated, with OCRs in the order of 1.1, which were measured by conducting odometer tests on undisturbed soil samples retrieved from each in situ soil layer. The groundwater table lies at a depth of 1.3 m below the ground surface. The secondary compression index is equal to 0.00595, and then the ratio of secondary compression index to reference volumetric strain is about 1 day (Sekiguchi 1984). The effective Poisson’s ratio of the surrounding clay can be assumed as 0.3. The plastic volumetric strain ratio, Λ , is taken

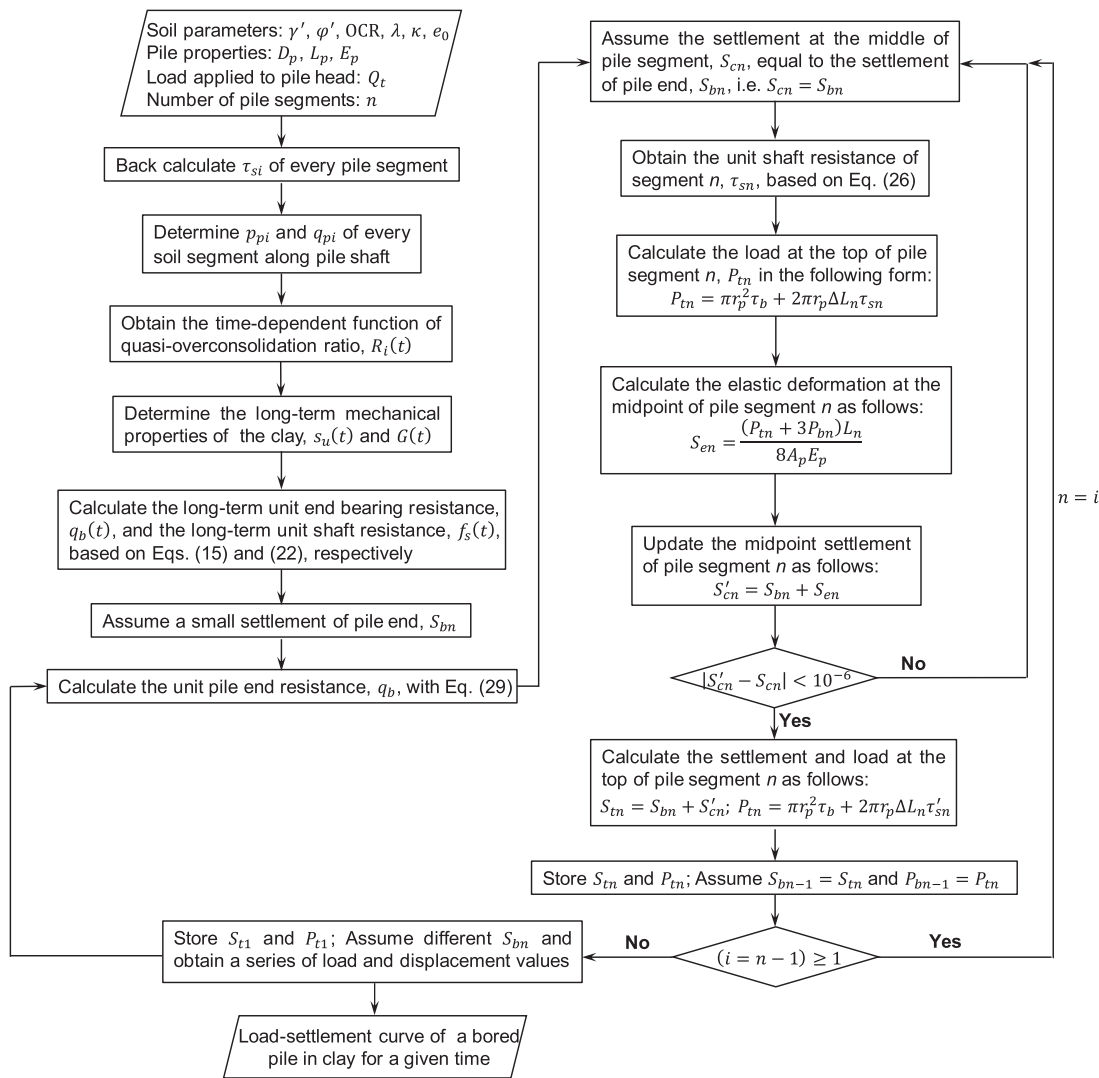


Fig. 8. Procedures for determining long-term load–settlement behavior of a pile in clay.

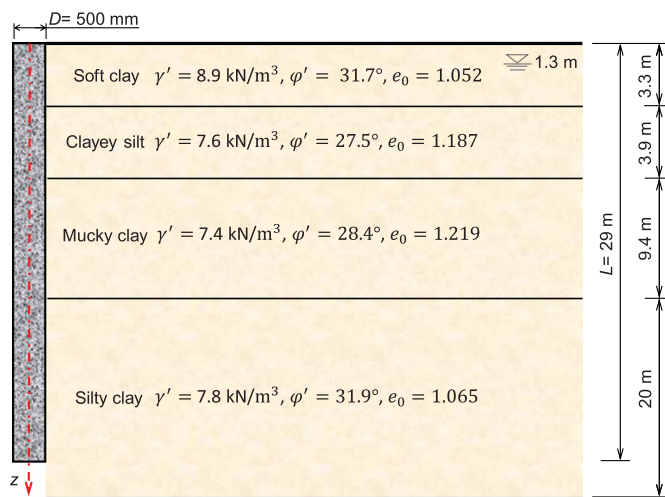


Fig. 9. Bored pile dimensions and soil files at the field test site.

as its typical value as 0.8 (Cao et al. 2001). Fig. 9 presents the soil profiles with the other measured soil properties along depth at the test site, which include the effective unit weight, effective internal friction angle, and the void ratio of each soil layer. The unit weights

of soils were determined through measuring the weights and volumes of soil samples obtained from a cutting ring. Then, the effective unit weight of each soil layer was obtained by subtracting the unit weight of water from the unit weight of soil. The void ratio was calculated based on the weight and the volume relationship by measuring the water contents and the specific gravities of soils via the oven drying method and the pycnometer method, respectively. The effective internal friction angle of each soil layer was measured from the triaxial compression tests on undisturbed soil samples from each soil layer. The coefficient of earth pressure at rest, K_0 , is estimated by the following equation (Mayne and Kulhawy 1982):

$$K_0 = (1 - \sin \varphi') \text{OCR}^{\sin \varphi'} \quad (37)$$

Fig. 10 shows the comparison between the predicted and measured load–settlement behaviors of the existing bored pile at the test site. It can be observed that the predicted load–settlement curve shows a good agreement with the measured values. Therefore, it proves reasonable to apply the proposed framework to explore the long-term load-carrying behavior of a bored pile in clay. To further examine the validity of the proposed analytical procedure for estimating load-carrying behavior of bored piles in clay, the field static load tests on two individual bored piles conducted by Dai et al. (2012) were selected for comparison. The reason for choosing the

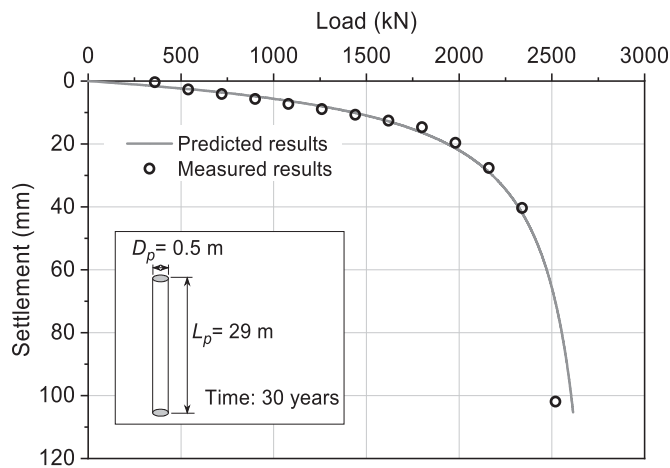


Fig. 10. Predicted and measured load–settlement curves of an existing pile at the field test site.

tests is that the information about the pile dimensions and soil parameters that need for calculation is relatively easy to find and the test procedure is also introduced in detail. The lengths of two single bored piles are 20 and 24 m, respectively, while the diameters of two piles are both 0.4 m. The elastic modulus of the pile concrete was measured as 29.2 GPa. Considering the contribution made by reinforcing bars, the elastic modulus of bored piles can be reasonably estimated as 35 GPa. The specific soil parameters can be found in Dai et al. (2012), except the overconsolidation ratio. The test site is located in the Qinhuai River floodplain, where the clay is generally the slightly or moderately overconsolidated clay. Therefore, three different OCRs, i.e., OCR=2, 3, 4, are adopted to predict the load–settlement behaviors of the two bored piles with different lengths, just as shown in Fig. 11. It can be seen from the figures that for the bored pile with the length of 20 m [i.e., Fig. 11(a)], the predicted curve with OCR=4 fits the measured test data best, while the predicted curve with OCR=4 for the bored pile with the length of 24 m [i.e., Fig. 11(b)] seems not to fit the measured result best, but the agreement is still acceptable. Hence, it can be initially assumed that the clay in the test site is the moderate overconsolidated clay, the OCR of which is equal to 4. In addition, it can be concluded that the proposed analytical procedure can also be employed to predict the load-carrying behavior of bored piles in clay immediately after the construction.

To better understand the load-carrying behaviors of existing bored piles, it is worth continuing to explore the load-carrying behaviors of the existing bored pile at the field test site, which here is assumed to have existed in the test site for different decades. It is interestingly seen in Fig. 12 that the pile stiffness increases significantly with time. However, the increase magnitude of the pile stiffness decreases as time goes on. When the existing time is over 60 years, the load–settlement curves of the pile are very close. On the other hand, the long-term load-carrying capacity of the bored pile is predicted as shown in Fig. 13. It can be easily observed that the load-carrying capacity of the bored pile increases much faster in the first 20 years and the increase magnitude is in the order of 74.2% of the initial load-carrying capacity, which accounts for the major growth of load-carrying capacity in 100 years. However, with the elapse of time, the increase magnitude decreases apparently, and in the last 20 years, it only accounts for 4.2% of the initial load-carrying capacity.

The reasons why the existing pile shows the aforementioned long-term load-carrying behaviors are illustrated in Fig. 14. Note that the soil element explored in the figures is close to the midpoint

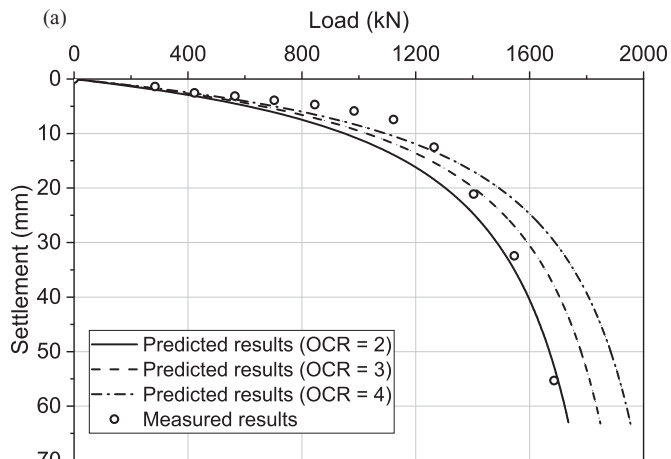
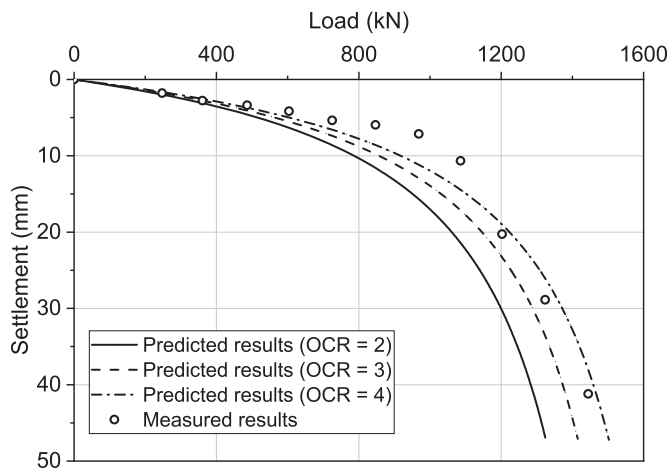


Fig. 11. Predicted and measured load–settlement curves of two bored piles from Dai et al. (2012): (a) pile length $L = 20$ m; and (b) pile length $L = 24$ m.

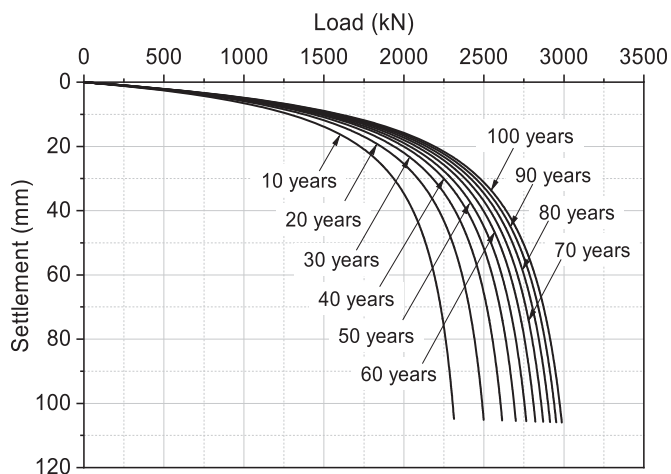


Fig. 12. Prediction of load–settlement curves of the bored pile existing at the field test site for different decades.

of the pile. Due to the creep of the clay around the bored pile, the quasi-overconsolidation ratio shows a faster increase trend at first and then a slower increase trend. When the existing time reaches 100 years, the increase magnitude of quasi-overconsolidation ratio is much smaller. This is because the creep rate of the

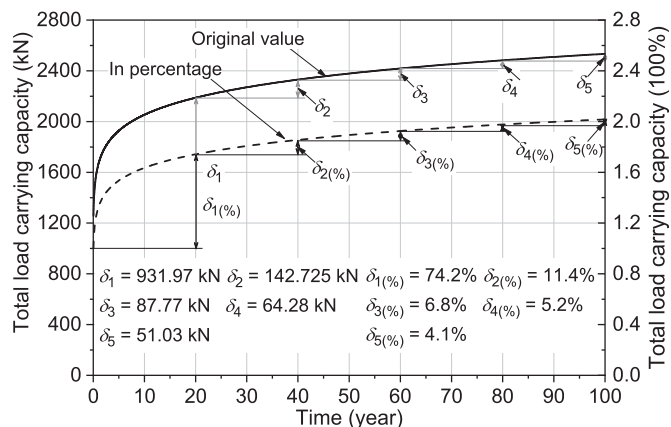


Fig. 13. Prediction of long-term load-carrying capacity of the bored pile existing at the field test site.

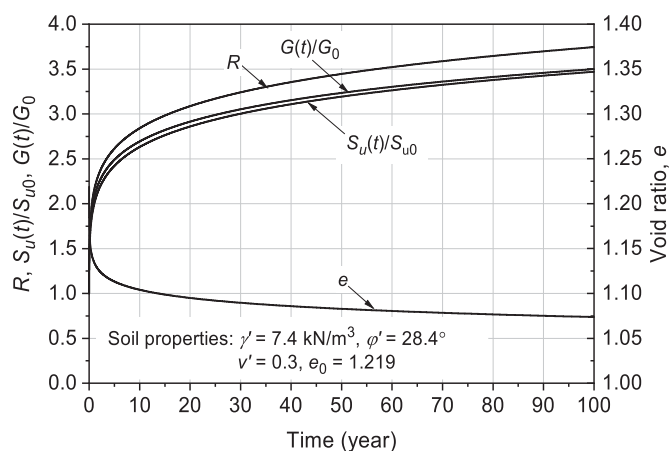


Fig. 14. Variation of quasi-overconsolidation ratio, undrained shear strength, shear modulus, and void ratio of clay at the field test.

surrounding clay is much larger in the beginning, but the creep rate decreases as time goes on. From Eq. (9), it can be seen that the undrained shear strength is in proportion to the quasi-overconsolidation ratio, so the undrained shear strength shows the similar variation trend as the quasi-overconsolidation ratio. Furthermore, the load-carrying capacity of a bored pile significantly depends on the undrained shear strength of the surrounding clay [see Eqs. (15) and (21)]. Hence, the loading-carrying capacity of the bored pile also first shows the faster increase trend and then the slower increase trend. This phenomenon is also shown in Fig. 15, which shows the variation of equivalent preconsolidation pressure and the corresponding yield surface. From the figure, it can be observed that with the passage of time, the equivalent preconsolidation pressure increases and the corresponding yield surface expands. They particularly increase and expand much faster in the first two decades and then the increase and expansion rates decrease. Correspondingly, it well depicts that the undrained shear strength of the surrounding clay increases much faster in the beginning and then the increase rate of undrained shear strength decreases, which appropriately explains the variation trend of the long-term load-carrying capacity of the bored pile as well.

Moreover, Fig. 14 illustrates that the void ratio decreases as time passes, which is induced by the creep of the surrounding clay. The shear modulus of the surrounding clay should have decreased due to the decrease of void ratio [see Eq. (13)]. However, the decrease

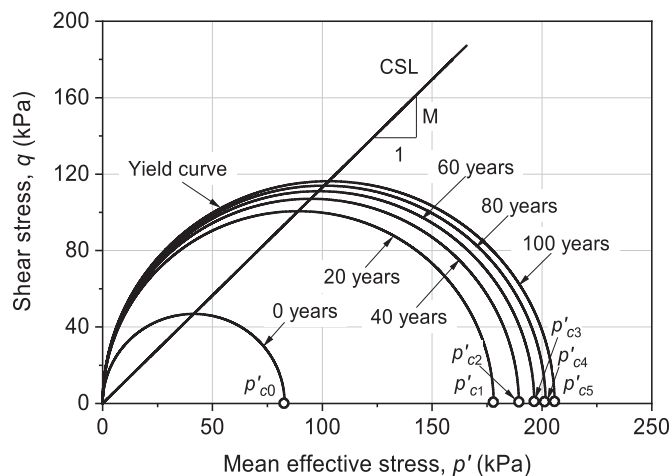


Fig. 15. Variation of equivalent preconsolidation pressure and corresponding yield surfaces of clay around the bored pile with respect to time.

Table 1. Clay parameters for parametric study

Soil parameter	Value
Effective unit weight, γ' (kN/m^3)	7.4
Effective Poisson's ratio, ν'	0.3
Effective internal friction angle, ϕ' ($^\circ$)	28.4
Slope of swelling line, κ	0.022
Plastic volumetric strain ratio, Λ	0.8
Initial void ratio, e_0	1.219
Overconsolidation ratio, OCR	1

magnitude of void ratio is much smaller than the increase magnitude of the quasi-overconsolidation ratio. Hence, the shear modulus of the surrounding clay still increases with time, and the variation trend is similar to the quasi-overconsolidation ratio. Consequently, a larger increase magnitude of pile stiffness occurs at first and then a smaller increase magnitude occurs, just like the comparison results of load–settlement behaviors of the bored pile existing for different decades, as shown in Fig. 12.

It is worth noting that although the increase magnitude of the load-carrying capacity of the bored pile existing for 100 years is much smaller when compared with the values of the first 20 years, it does not reach a value close to 0. The reason is that the creep of a clay generally lasts for thousands of years. The creep rate of the clay is still relatively large; even it has undergone one-hundred-year creep. However, 100 years are enough for exploring the long-term load-carrying behaviors of a bored pile in clay.

Parametric Study

Effects of Secondary Compression Index

It can be seen from Eq. (7) that the secondary compression index is a significant parameter that affects the magnitude of the quasi-overconsolidation ratio and further exerts influences on the long-term load-carrying behaviors of a bored pile in clay. Hence, three different values of secondary compression index, which are 0.006, 0.005, and 0.004, are adopted to explore its effects on load-carrying behaviors of bored piles in clay. Table 1 summarizes the soil parameters used for the parametric study. Fig. 16 shows the effects of the secondary compression index on the quasi-overconsolidation ratio. It depicts that the quasi-overconsolidation ratio increases with

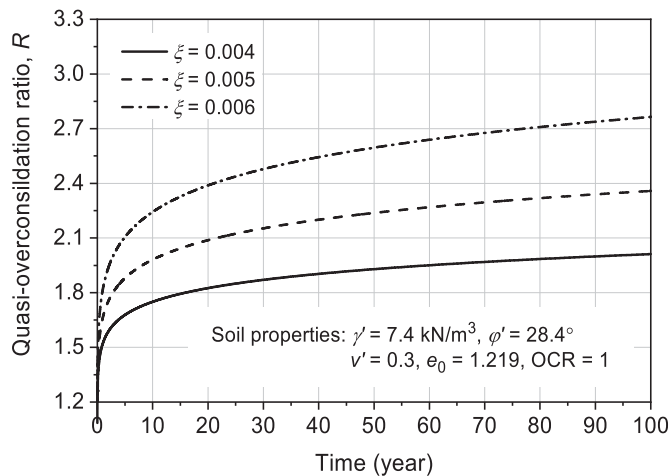


Fig. 16. Effects of secondary compression index on the quasi-overconsolidation ratio.

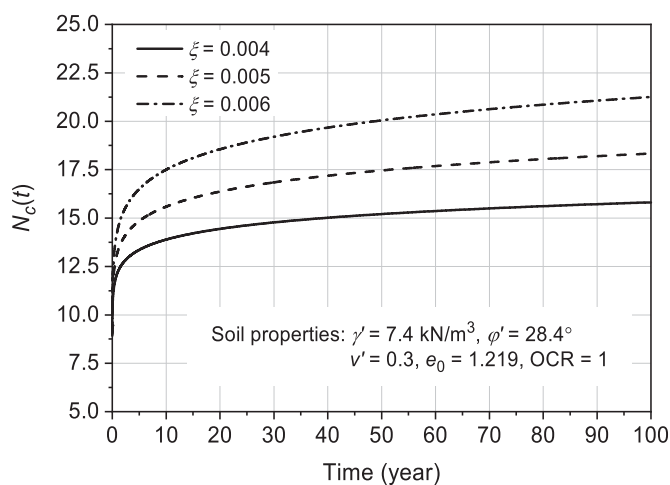


Fig. 17. Effects of secondary compression index on the long-term pile end load-carrying capacity factor.

the increase of the secondary compression index. Moreover, the quasi-overconsolidation ratio with a larger secondary compression index increases much faster than that with a smaller one. In other words, it costs less time for the quasi-overconsolidation ratio with a smaller secondary compression index to reach a constant value.

The long-term pile end bearing capacity factor and the long-term pile shaft resistance factor serve as the two key factors that affect the long-term load-carrying behaviors of a bored pile in clay. The effects of the secondary compression index on them are shown in Figs. 17 and 18. Similarly, the values and the increase rates of both two factors with a larger secondary compression index are larger than those with a smaller one. This indicates that the bored pile in clay with a smaller secondary compression index needs less time to reach a constant load-carrying capacity and its long-term load-carrying capacity is less than that of the bored pile in clay with a larger secondary compression index. To well illustrate this statement, the effects of secondary compression index on the total long-term load-carrying capacity of a bored pile with the length of 29 m and the diameter of 500 mm are shown in Fig. 19. Note that here the soil stratum is assumed to only consist of one kind of soil, the mechanical parameters of which are the same as those in Table 1. It can be seen from Fig. 19 that the load-carrying capacity of bored piles in

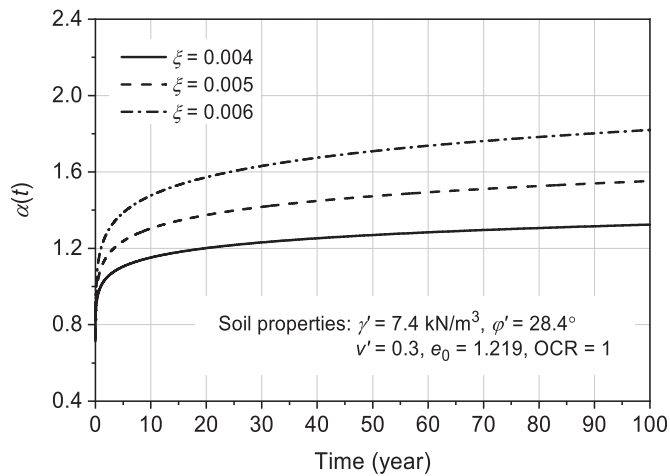


Fig. 18. Effects of secondary compression index on the long-term pile shaft resistance factor.

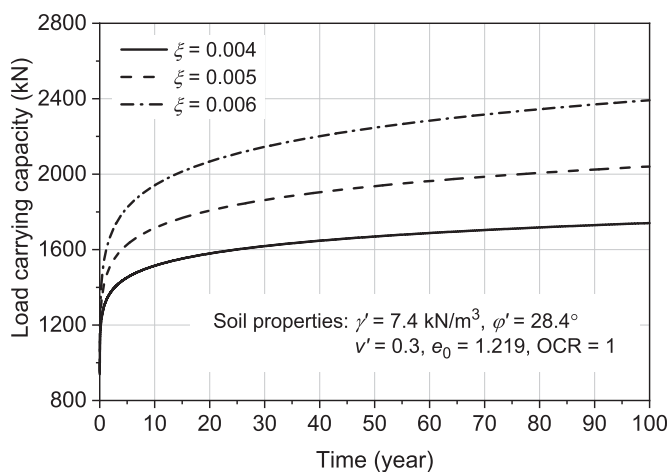


Fig. 19. Effects of secondary compression index on the long-term load-carrying capacity.

soil with a larger secondary compression index increases more rapidly than bored piles in soils with smaller secondary compression indices, and it costs much less time for the load-carrying capacity of bored piles in soil with a smaller secondary compression index to reach a constant load-carrying capacity. Therefore, this phenomenon strongly supports the results summarized from the analysis on the effects of secondary compression index on the long-term pile end bearing capacity factor and the long-term pile shaft resistance factor.

Effects of In Situ Soil Properties

Most in situ clays are found in different consolidation states and in another word own different OCRs. The OCR not only has vital effects on the soil behaviors, but also possesses the feature that is independent of other soil parameters, which makes it more proper than the other soil parameters to be used in the parametric studies. Hence, the in situ OCR is chosen as a representative parameter to explore the effects of in situ soil properties on the long-term load-carrying behaviors of bored piles. Here, three different OCRs (i.e., 1, 2, and 4) are used to represent the in situ clays with different consolidation degrees, i.e., normally consolidated clay, slightly overconsolidated clay, and moderately overconsolidated clay. The coefficients of earth pressure at rest are also

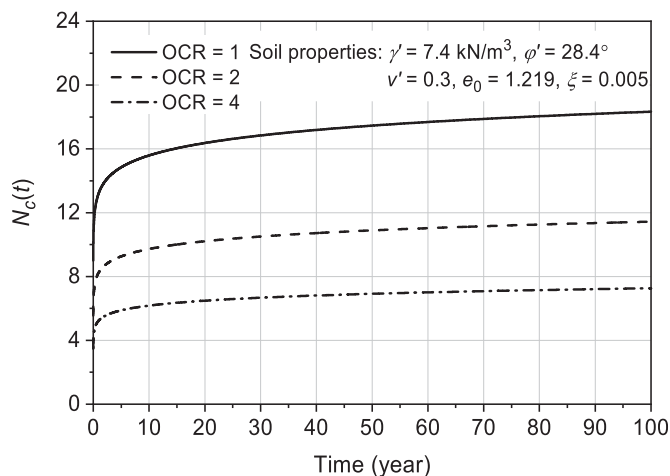


Fig. 20. Effects of overconsolidation ratio on the long-term end load-carrying capacity factor.

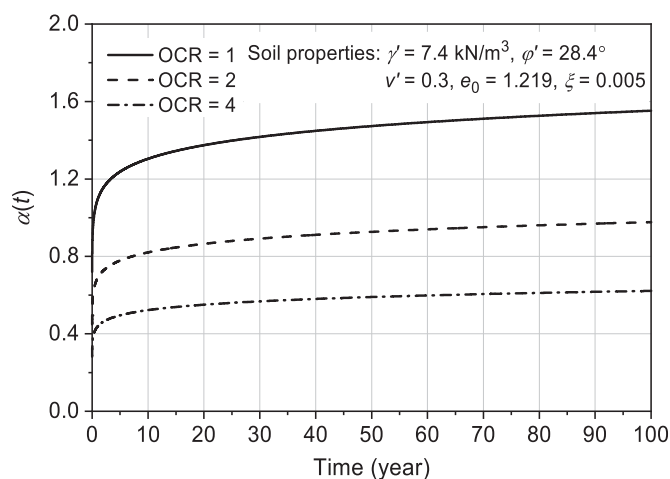


Fig. 21. Effects of overconsolidation ratio on the long-term pile shaft resistance factor.

estimated based on Eq. (37). Note that the other soil parameters required in this analysis are the same as those tabulated in Table 1, except that $\xi = 0.005$ should replace OCR = 1 in the table.

It can be observed from Figs. 20 and 21 that, for normally consolidated clay, both the long-term pile end bearing capacity factor and the long-term pile shaft resistance factor increase much faster than those of the clays with different consolidation degrees. However, it is much quicker for the two bearing capacity factors of the clay with larger OCRs to reach constant values. Here, it should be noted that the bored pile in the normally consolidated clay owns the largest bearing capacity factors. To better illustrate the effects of OCR, Fig. 22 plots the long-term load-carrying capacity of a bored pile in soils with these three different OCRs, respectively. It can be observed that although the bearing capacity factors of bored piles in soils with larger OCRs reach constant values more quickly, the load-carrying capacity of bored piles in normally consolidated clay reaches the constant capacity more rapidly. Besides, it is interestingly observed that the bored pile in the moderately overconsolidated soil owns the largest load-carrying capacity, which is different from the phenomenon observed in the analysis of the effects of OCR on two bearing capacity factors. The reasons for these two phenomena observed in Fig. 22 are the same, which is that soils with larger OCRs generally possess larger undrained shear strength

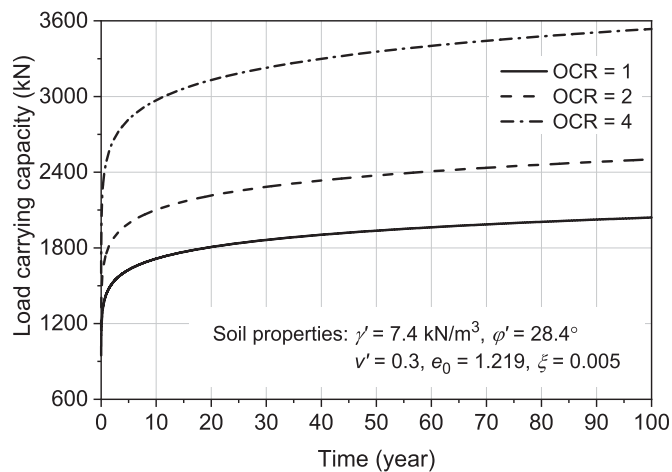


Fig. 22. Effects of overconsolidation ratio on the long-term load-carrying capacity.

that has strong effects on the load-carrying capacity of bored piles in clay.

Discussions

When employing existing piles to construct pile foundations with new piles, there are some potential difficulties and challenges we may be faced with. The specific difficulties and challenges mainly include the durability, the disturbance caused by new pile construction, and the load-carrying behavior of existing piles incapable of meeting the requirement of constructing new buildings. Because existing piles have generally existed in the construction sites for many years, they may have suffered a certain degree of corrosion attack and their service life is likely not so long as that of new piles. In other words, the service life of pile foundations may be reduced to a certain degree if employing existing piles to construct it. Besides, some disturbances can be caused on the existing piles when constructing new piles and, as a result, adversely affect the load-carrying behavior of existing piles. Specifically, when the new piles are chosen as jacked piles, this pile type has a chance to result in great disturbance on existing piles. Moreover, the new buildings usually have larger weights that need the pile foundation to support than the demolished buildings. Therefore, new piles with larger dimensions are needed to offer more load-carrying capacities, which indicate that the existing piles with the determined dimensions may be unable to offer such high load-carrying capacities and, consequently, cannot be reused for constructing new buildings. In general, reusing existing piles is a comprehensive but complex problem. Except for the aforementioned difficulties and challenges, some other difficulties and challenges that the authors have not covered should also be taken into consideration so as to better and more safely reuse existing piles.

It is worth noting that the proposed analytical method can be extended to predict the long-term load-carrying capacity of driven piles in clay through incorporating the effects of dissipation of excess pore-water pressures that are generated during the installation of driven piles. Compared with the construction effects of bored piles, the construction of driven piles always gives rise to excess pore-water pressures in the clay adjacent to piles. Therefore, when exploring the long-term load-carrying capacity of bored piles in clay, both the effects of excess pore-water pressure and the clay creep should be taken into account. Generally, the dissipation of excess pore-water pressures only lasts for tens of days or several months. In addition, although the clay creep also occurs during the

dissipation of excess pore-water pressure, the effects in this period prove to be negligible (Bullock et al. 2005a, b; Augustesen 2006). Hence, these two effects can be separately considered on the long-term load-carrying capacity of driven piles. The effects of excess pore-water pressures on driven piles were explored in detail by Li et al. (2017a), which can serve for a reference method to investigate the effects of excess pore-water pressures. Then, combined with the proposed method, the long-term load-carrying capacity of driven piles can be finally predicted.

Compared with the previous studies, the differences and innovations of present study can be summarized as follows: (1) The previous studies only focus on the short-term limiting load-carrying capacity and load–displacement behavior of piles, while the present study aims at exploring and predicting not only the long-term load-carrying capacity, but also the long-term load–settlement behavior of bored piles in clay through taking the creep behavior of surrounding clay into account based on the elasto-viscoplastic constitutive model. (2) The methods (load-transfer method) of previous studies were used in this study to determine the stress states of surrounding clay to simulate and analyze its creep behavior. From this point of view, the load-transfer method adopted from the previous studies is only a small part of the current study, although it is an essential part to assist in analyzing the long-term load-carrying behavior of bored piles in clay. (3) The key innovation of the present study is that the creep behaviors of surrounding clay are modeled and incorporated in the load-transfer functions to predict the long-term load-carrying behavior of bored piles. Because the long-term load-carrying behavior of bored piles primarily depends on the long-term properties of surrounding clay, the proposed load-transfer curves could yield reasonable predictions. (4) The code of proposed analytical procedure is developed for predicting the long-term load-carrying behavior of bored piles in clay, which could help geotechnical engineers efficiently and easily determine the long-term load-carrying behavior of bored piles. Moreover, making use of the developed code, a comprehensive parametric study has also been conducted to illustrate the important factors that may significantly affect the long-term load-carrying behavior of bored piles. All of these efforts can provide important guidance for geotechnical engineers when planning to reuse existing bored piles.

Conclusions

In this paper, an analytical framework is developed to explore the long-term load-carrying behaviors of a bored pile in clay, so as to achieve the aim of reusing existing bored piles. The predicted results are compared with a pile field test conducted by the authors and field static load tests on two single bored piles conducted by other researchers to verify the proposed framework and are extended to investigate the long-term load-carrying behaviors of the existing bored pile. Parametric studies are performed to analyze the influences of significant soil parameters on the long-term load-carrying behaviors of a bored pile in clay. The potential difficulties and challenges lying in reusing existing piles as well as the innovations of this study are discussed in detail. The results drawn from this study are briefly summarized in the following:

1. The present analytical procedure can be reasonably applied to predict the long-term load-carrying behaviors of a bored pile in clay. It shows a satisfactory agreement between the predicted and measured results. It is worth pointing out that the unloading–reloading effect of the existing bored pile has not been considered in this study, because the effect in the field test was not very significant. However, if this effect shows strong influences, it should be taken into account when trying to understand the

load-carrying behaviors of existing bored piles in clay. To the best of the authors' knowledge, the unloading and reloading effect of existing bored piles has not been explored yet; hence, it can be the next important research topic after this paper.

2. Due to the clay creep, the undrained shear strength and the shear modulus of the clay around bored piles increase with the elapse of time, but the increase magnitudes decrease as time further goes on. Thus, the pile stiffness increases with time, but the increase magnitude decreases with the elapse of time. Moreover, the load-carrying capacity of bored piles increases much faster in the first several decades, but it will nearly reach a constant value when time is long enough.
3. The secondary compression index and the in situ overconsolidation ratio significantly affect the long-term load-carrying behaviors of bored piles in clay. The bored pile in clay with a large secondary compression index or week consolidation degree costs less time to reach a constant load-carrying capacity.

Data Availability Statement

Some or all data, models, or code generated or adopted in this study are available from the corresponding author upon reasonable request.

Acknowledgments

This study was financially supported by the National Natural Science Foundation of China (Grant No. 41772290).

References

- Ashour, M., G. M. Norris, S. Elfass, and A. Z. Al-Hamdan. 2010. "Mobilized side and tip resistances of piles in clay." *Comput. Geotech.* 37 (7–8): 858–866. <https://doi.org/10.1016/j.compgeo.2010.07.005>.
- Augustesen, A. 2006. "The effects of time on soil behaviour and pile capacity." Ph.D. thesis, Dept. of Civil Engineering, Aalborg Univ.
- Augustesen, A., M. Liingaard, and P. V. Lade. 2004. "Evaluation of time-dependent behavior of soils." *Int. J. Geomech.* 4 (3): 137–156. [https://doi.org/10.1061/\(ASCE\)1532-3641\(2004\)4:3\(137\)](https://doi.org/10.1061/(ASCE)1532-3641(2004)4:3(137)).
- Basu, P., M. Prezzi, R. Salgado, and T. Chakraborty. 2014. "Shaft resistance and setup factors for piles jacked in clay." *J. Geotech. Geoenviron. Eng.* 140 (3): 0401302. [https://doi.org/10.1061/\(ASCE\)GT.1943-5606.0001018](https://doi.org/10.1061/(ASCE)GT.1943-5606.0001018).
- Bjerrum, L. 1967. "Engineering geology of Norwegian normally-consolidated marine clays as related to settlements of buildings." *Géotechnique* 17 (2): 83–118. <https://doi.org/10.1680/geot.1967.17.2.83>.
- Bullock, P. J., J. H. Schmertmann, M. C. McVay, and F. C. Townsend. 2005a. "Side shear setup. I: Test piles driven in Florida." *J. Geotech. Geoenviron. Eng.* 131 (3): 292–300. [https://doi.org/10.1061/\(ASCE\)1090-0241\(2005\)131:3\(292\)](https://doi.org/10.1061/(ASCE)1090-0241(2005)131:3(292)).
- Bullock, P. J., J. H. Schmertmann, M. C. McVay, and F. C. Townsend. 2005b. "Side shear setup. II: Results from Florida test piles." *J. Geotech. Geoenviron. Eng.* 131 (3): 301–310. [https://doi.org/10.1061/\(ASCE\)1090-0241\(2005\)131:3\(301\)](https://doi.org/10.1061/(ASCE)1090-0241(2005)131:3(301)).
- Cao, L. F., C. I. Teh, and M. F. Chang. 2001. "Undrained cavity expansion in modified Cam clay I: Theoretical analysis." *Geotechnique* 51 (4): 323–334.
- Dai, G., R. Salgado, W. Gong, and Y. Zhang. 2012. "Load tests on full-scale bored pile groups." *Can. Geotech. J.* 49 (11): 1293–1308. <https://doi.org/10.1139/t2012-087>.
- Flaate, K. 1972. "Effects of pile driving in clays." *Can. Geotech. J.* 9 (1): 81–88. <https://doi.org/10.1139/t72-006>.

- Guo, W. D. 2000. "Visco-elastic consolidation subsequent to pile installation." *Comput. Geotech.* 26 (2): 113–144. [https://doi.org/10.1016/S0266-352X\(99\)00028-2](https://doi.org/10.1016/S0266-352X(99)00028-2).
- Lam, C., and S. A. Jefferis. 2011. "Critical assessment of pile modulus determination methods." *Can. Geotech. J.* 48 (10): 1433–1448. <https://doi.org/10.1139/t11-050>.
- Li, L., J. Li, D. A. Sun, and W. Gong. 2017a. "Analysis of time-dependent bearing capacity of a driven pile in clayey soils by total stress method." *Int. J. Geomech.* 17 (7): 04016156. [https://doi.org/10.1061/\(ASCE\)GM.1943-5622.0000860](https://doi.org/10.1061/(ASCE)GM.1943-5622.0000860).
- Li, L., J. Li, D. A. Sun, and W. Gong. 2017b. "Semi-analytical approach for time-dependent load–settlement response of a jacked pile in clay strata." *Can. Geotech. J.* 54 (12): 1682–1692. <https://doi.org/10.1139/cgj-2016-0561>.
- Li, L., J. Li, D. A. Sun, and L. Zhang. 2017c. "Time-dependent bearing capacity of a jacked pile: An analytical approach based on effective stress method." *Ocean Eng.* 143: 177–185. <https://doi.org/10.1016/j.oceaneng.2017.08.010>.
- Matsuoka, H., and D. Sun. 2006. *The SMP concept-based 3D constitutive models for geomaterials*. Leiden, Netherlands: Taylor & Francis.
- Matsuoka, H., Y.-P. Yao, and D. Sun. 1999. "The Cam-clay models revised by the SMP criterion." *Soils Found.* 39 (1): 81–95. <https://doi.org/10.3208/sandf.39.81>.
- Mayne, P. W., and F. H. Kulhawy. 1982. " K_0 -OCR relationship in soil." *J. Geotech. Eng. Div.* 108 (6): 851–872.
- O'Neil, M. W., and L. C. Reese. 1999. *Drilled shafts: Construction procedures and design methods*. FHA Publication No. FHWA-IF-99-025. Washington, DC: US Department of Transportation.
- Randolph, M. F., and C. P. Wroth. 1979a. "An analytical solution for the consolidation around a driven pile." *Int. J. Numer. Anal. Methods Geomech.* 3 (3): 217–229. <https://doi.org/10.1002/nag.1610030302>.
- Randolph, M. F., and C. P. Wroth. 1979b. "An analysis of the vertical deformation of pile groups." *Géotechnique* 29 (4): 423–439. <https://doi.org/10.1680/geot.1979.29.4.423>.
- Randolph, M. F., and C. P. Wroth. 1981. "Application of the failure state in undrained simple shear to the shaft capacity of driven piles." *Géotechnique* 31 (1): 143–157. <https://doi.org/10.1680/geot.1981.31.1.143>.
- Roy, M., and M. Lemieux. 1986. "Long-term behaviour of reconsolidated clay around a driven pile." *Can. Geotech. J.* 23 (1): 23–29. <https://doi.org/10.1139/t86-004>.
- Schmertmann, J. H. 1991. "The mechanical aging of soils." *J. Geotech. Eng.* 117 (9): 1288–1330. [https://doi.org/10.1061/\(ASCE\)0733-9410\(1991\)117:9\(1288\)](https://doi.org/10.1061/(ASCE)0733-9410(1991)117:9(1288)).
- Sekiguchi, H. 1984. "Theory of undrained creep rupture of normally consolidated clay based on elasto-viscoplasticity." *Soils Found.* 24 (1): 129–147. <https://doi.org/10.3208/sandf1972.24.129>.
- Tavenas, F., and R. Audy. 1972. "Limitations of the driving formulas for predicting the bearing capacities of piles in sand." *Can. Geotech. J.* 9 (1): 47–62. <https://doi.org/10.1139/t72-004>.
- Wardle, I. F., G. Price, and J. Freeman. 1992. "Effect of time and maintained load on the ultimate capacity of pile in stiff clay." In *Proc., Piling: European Practice and Worldwide Trends*, 92–99. London: The Institution of Civil Engineers.
- Wood, D. M. 1990. *Soil behaviour and critical state soil mechanics*. Cambridge, UK: Cambridge University Press.
- Xia, Z., and J. Zou. 2017. "Simplified approach for settlement analysis of vertically loaded pile." *J. Eng. Mech.* 143 (11): 04017124. [https://doi.org/10.1061/\(ASCE\)EM.1943-7889.0001334](https://doi.org/10.1061/(ASCE)EM.1943-7889.0001334).
- Yao, Y. P., W. Hou, and A. N. Zhou. 2009. "UH model: Three-dimensional unified hardening model for overconsolidated clays." *Géotechnique* 59 (5): 451–469. <https://doi.org/10.1680/geot.2007.00029>.
- Zhang, Q., and Z. Zhang. 2012. "Simplified calculation approach for settlement of single pile and pile groups." *J. Comput. Civ. Eng.* 26 (6): 750–758. [https://doi.org/10.1061/\(ASCE\)CP.1943-5487.0000167](https://doi.org/10.1061/(ASCE)CP.1943-5487.0000167).
- Zhao, C. F., J. Lu, Q. C. Sun, T. Zhu, and S. F. Li. 2009. "Experimental study of load transmission property of large-diameter bored cast-in-situ deep and long pile in different soil layers." [In Chinese.] *Chin. J. Rock Mech. Eng.* 28 (5): 1020–1026.